International Journal of Power Electronics and Drive System (IJPEDS)
Vol. 16, No. 4, December 2025, pp. 2321~2331
ISSN: 2088-8694, DOI: 10.11591/ijpeds.v16.i4.pp2321-2331

Improvement of DSIM control using fuzzy third-order sliding mode approach optimized by MOA

Rahma Belkaid[1], Lamia Youb[1], Farid Naceri[1], Ghoulem Allah Boukhalfa[2]
[1]Electrical Traction Systems Laboratory, Department of Electrical Engineering, University of Batna 2 (Mostefa Ben Boulaid), Batna, Algeria
[2]Department of Electrical Engineering, University of Batna 2 (Mostefa Ben Boulaid), Batna, Algeria

Article Info

Article history:

Received Jan 31, 2025
Revised Sep 23, 2025
Accepted Oct 2, 2025

Keywords:

Dual-star induction motor
Fuzzy logic
Fuzzy third-order sliding mode controller
Mayfly optimization algorithm
Sliding mode technique

ABSTRACT

This study focuses on the contribution of a new hybrid controller based on the sliding mode technique associated with fuzzy logic and optimized by an innovative approach called the mayfly optimization algorithm (MOA) to improve the drive of the dual star induction motor (DSIM). The performance and robustness of this system are analyzed under different operating conditions with three proposed strategies and compared with each other under the MATLAB/Simulink environment. Through the simulation results obtained, we realize that the method that integrates the MOA with a hybrid controller associating the third-order sliding mode with fuzzy logic (MOA-FTOSMC) makes a significant contribution to research work in this field and offers the best dynamic performance and adequately manages the uncertainty and variation of the system parameters under different operating regimes.

This is an open access article under the CC BY-SA license.

Corresponding Author:

Rahma Belkaid
Electrical Traction Systems Laboratory, Department of Electrical Engineering
University of Batna 2 (Mostefa Ben Boulaid)
Batna, Algeria
Email: rahma.belkaid@univ-batna2.dz

1. INTRODUCTION

The dual-star induction motor is currently attracting increasing interest in high-power applications due to the accessibility of its rotor and the remarkable performances it develops with vector control techniques. It is usually made up of two sets of windings to operate at low and high voltage [1], [2]. This versatility gives it a certain flexibility and allows it to be used in different environments and with different energy sources [3]. The vector control technique was developed in the early 1970s by Blaschke and is based on classical speed regulators (proportional, integral, and derivative (PID) regulators). However, this technique has difficulties in controlling transient speeds and parametric variations of the machine; in order to overcome this handicap, researchers have introduced artificial intelligence techniques in order to better adapt it to these requirements [4]. In order to judiciously adjust the PID factors and optimize the performance of the control system, various nature-inspired algorithms have been proposed in recent years. Particle swarm optimization (PSO) algorithm, simulated annealing (SA), atom search (ASO), genetic algorithm (GA), and firefly algorithm (FA). All these approaches aim to achieve optimum accuracy in trajectory tracking [5]-[7]. Many studies have shown that PSO hybrid controllers associated with fuzzy logic controllers encounter difficulties in various applications to optimize the gains Kp and Ki of the classic PI speed regulator and obtain better regulation accuracy [8]. However, the advantages of the fuzzy sliding mode control strategy based on an innovative optimization algorithm called MOA substituted for the speed regulator prove to be more interesting in terms of performance and robustness [9]. MOA is a bio-inspired optimization method based on the behavior of mayflies in nature. In

this algorithm, a population of virtual "flies" is used to explore the search space for optimal solutions to a given problem [10], [11]. This MOA is distinguished by the reduction of the number of iterations, the reduction of the risk of overfitting, and finally the avoidance of premature convergence, which results in convergence towards a local solution rather than a desired global solution [12], [13].

Sliding mode control (SMC) is a robust control technique for stabilizing dynamic systems [14], [15]. Its fundamental principle is to create a sliding surface in the system state space [16], [17], ensuring the motion toward a desired equilibrium. The sliding surface of SOSMC improves control accuracy and disturbance rejection [18]-[20]. TOSMC further incorporates third-order derivatives for higher accuracy and stability. These methods increase the complexity; however, their robust performance makes them suitable for applications requiring high accuracy and stability [21]-[25].

The objective of this work is to compare three innovative strategies of the DSIM drive under extreme operating conditions, in order to determine the technique that provides better energy efficiency and reduced losses for industrial applications. The simulation results under MATLAB/Simulink clearly illustrate the superiority of the MOA-FTOSMC technique, showing strong robustness against speed variations and a considerable reduction of the chattering phenomenon. The analysis also indicates that this strategy achieves the lowest harmonic distortion of the stator current (THD). Furthermore, it successfully minimizes the error criteria (ITAE, ITSE, and ISE), confirming its effectiveness in improving dynamic responses. In addition, the optimization process demonstrates that the MAO algorithm combined with the FTSOSMC regulator converges rapidly toward the optimal solution with fewer iterations, reinforcing the contribution of this approach compared to previously reported studies.

Table 1. Performance comparison for speed reversal

Approach	IAE	ISE	ITSE
MOA-SOSMC	62.90	4798	1.914e+04
MOA-TOSMC	39.713	4166	1.602e+04
MOA-FTOSMC	31.88	4035	1.401e+04

2. MATHEMATICAL MODEL OF DSIM

The dynamic equations of the DSIM can be reported in (d, q) axes as (1) [5], [6].

$$\begin{cases} V_{ds1} = R_{s1} i_{ds1} + \dfrac{d\varphi_{ds1}}{dt} - \omega_s \varphi_{qs1} \\ V_{qs1} = R_{s1} i_{qs1} + \dfrac{d\varphi_{qs1}}{dt} - \omega_s \varphi_{ds1} \\ V_{ds2} = R_{s1} i_{ds2} + \dfrac{d\varphi_{ds2}}{dt} - \omega_s \varphi_{qs2} \\ V_{qs2} = R_{s2} i_{qs2} + \dfrac{d\varphi_{qs2}}{dt} - \omega_s \varphi_{ds2} \\ V_{dr} = 0 = R_r i_{dr} + \dfrac{d\varphi_{dr}}{dt} + (\omega_s - \omega_r)\varphi_{qr} \\ V_{qr} = 0 = R_r i_{qr} + \dfrac{d\varphi_{qr}}{dt} + (\omega_s - \omega_r)\varphi_{dr} \end{cases} \quad (1)$$

For studying the dynamic behavior, the (2) of motion is added.

$$J\frac{d\Omega_r}{dt} = T_{em} - T_r - f_r \Omega_r \quad (2)$$

The model of the DSIM has been completed by the expression of the electromagnetic torque T_{em} given as (3).

$$T_{em} = p\frac{Lm}{L_m + L_r}\left(\varphi_{dr}(i_{qs1} + i_{qs2}) - \varphi_{qr}(i_{ds1} + i_{ds2})\right) \quad (3)$$

3. MATHEMATICAL MODEL OF IFOC

Indirect vector control is a technique that relies on classical PI-type regulators. However, these PI regulators encounter difficulties in adjusting the gains due to the non-linearity and the high complexity of the system [21]. In the application of IFOC to a DSIM, the "d" axis of the frame (dq) is aligned with the rotor flux, with:

$$\varphi_{qr} = 0 ; \varphi_{dr} = \varphi_r \quad (4)$$

The torque is (5).

$$C_{em} = P\frac{L_m}{L_m+L_r}[(i_{sq1} + i_{sq2})\varphi_r] \quad (5)$$

Then we can have the reference voltages $V_{ds1}{}^*$, $V_{qs1}{}^*$, $V_{ds2}{}^*$, $V_{qs2}{}^*$ based on DSIM.

$$\begin{cases} v^*_{sd1=} = R_{s1}i_{sd1} + L_{s1}\dfrac{d}{dt}i_{sd1} - w^*_s(L_{s1}i_{sq1} + T_r\varphi^*_r w^*_{gl}) \\ v^*_{sq1=} = R_{s1}i_{sq1} + L_{s1}\dfrac{d}{dt}i_{sq1} - w^*_s(L_{s1}i_{sd1} + \varphi^*_r) \\ v^*_{sd2=} = R_{s2}i_{sd2} + L_{s2}\dfrac{d}{dt}i_{sd2} - w^*_s(L_{s2}i_{sq2} + T_r\varphi^*_r w^*_{gl}) \\ v^*_{sq2} = R_{s2}i_{sq2} + L_{s2}\dfrac{d}{dt}i_{sq2} - w^*_s(L_{s2}i_{sd2} + \varphi^*_r) \end{cases} \quad (6)$$

The orientation angle $\theta_{\varphi r\_est}$ are (7).

$$\theta_{\varphi r\_est} = \tan^{-1}\frac{d\varphi_{dr\_est}}{\varphi_{qr\_est}} \quad (7)$$

4. PRESENTATION OF MAYFLY OPTIMIZATION ALGORITHM TECHNIQUE

The MOA was established by Zervoudakis and Tsafarakis [10]; it presents a combination of classical optimization methods such as PSO, GA, and the Firefly algorithm. It is able to provide a robust approach to adjust the best gains k_i and k_p of a speed controller in a double-star induction machine drive system. The appropriate combination of these three optimization strategies aims to overcome the shortcomings that may hinder the use of a single algorithm to some extent and to enhance the capabilities of the combined algorithm to improve its performance [12]. MOA is an efficient and innovative tool inspired by the migratory behavior of mayflies. It is used to simulate foraging and reproduction and to refine the best solutions found by GA, focusing on exploring the solution space and identifying promising configurations [26]. The objective function f(x) defined beforehand determines the optimization of the algorithm in the form of a solution of f(x) represented by an n-dimensional vector x = (x1, x2, x3,..., xn) composed of two swarms of female and male mayflies whose movement of each of them is represented by a speed v = (v1, v2, v3,….., xd). The personal and community characteristics and interactions specific to each mayfly lead it to modify its trajectory during its flight in order to covet its best location, which is in fact that of the swarm [26]. The different steps to implement the mayfly optimization algorithm are initialization by generating a male and female population, respectively, from the x = (x1,…, xd) and y = (y1,…, yd), where their speed is updated by the equation v = (v1,…, vd).

5. HYBRID FUZZY THIRD ORDER SLIDING MODE CONTROL

In order to improve the robustness and stability of the DSIM-IFOC control, the speed regulator has been replaced by an improved controller, which is a hybrid TOSMC associated with FL. We have chosen for our study the TOSMC, which is a strategy that largely exceeds the limits of the classical SMC and is considered very effective for uncertain systems; its capabilities are close to those of the super torsion algorithm (STA) which is a unique high-order sliding mode control technique [17]. To improve the performance of the TOSMC method, it is necessary to appropriately choose the parameters (α_1,α_2,α_3) in order to judiciously exploit the Lyapunov criterion and thus influence the dynamics of the system to obtain a response speed with a record time, rigorous stability, and very satisfactory robustness to disturbances. The optimization method best suited to this iterative process is illustrated by the MOA, which has the advantage of combining GA, PSO, and FA to reduce the cost function and thus promote the best control of rise time, overshoot, and tracking [26]. The control input of the designed TOSM controller consists of three inputs given by the (8)-(11) [25].

$$U(t) = U_1(t) + U_2(t) + U_3(t) \quad (8)$$

$$U_1(t) = \alpha_1.\sqrt{|S_\Omega|}.\mathrm{Sign}(S_\Omega) \quad (9)$$

$$U_2(t) = \alpha_2.\int \mathrm{Sign}(S_\Omega)dt \quad (10)$$

$$U_3(t) = \alpha_3.\mathrm{Sign}(S_\Omega) \quad (11)$$

The (12) shows the output of the proposed TOSMC method:

$$U(t) = \alpha_1 . \sqrt{|S_\Omega|} . \text{Sign}(S_\Omega) + \alpha_2 . \int \text{Sign}(S_\Omega) dt + \alpha_3 . \text{Sign}(S_\Omega) \quad (12)$$

The TOSMC always remains ineffective in the face of the discontinuous term in the global control law, which introduces a chattering phenomenon [25]. To eliminate the undesirable effects of this phenomenon, we propose the contribution of fuzzy logic, which proves to be a strategy whose characteristics have been proven more particularly in the field of training electrical machines. The proposed fuzzy-sliding controller has the same control law as the TOSMC; however, the components, β_1 ,β_2 and β_3 have been adapted by a fuzzy inference table, which selects the adequate combination that converges the sliding fuzzy controller towards the desired sliding surface when the gains are adjusted to small values.

This suggested FTOSMC method was used to improve the performance of the IFOC method by refining the TOSM strategy using fuzzy logic and ensuring the smoothing of the hybrid controller [23], [24]. The stability condition is given by (13).

$$S\dot{S}<0 \quad (13)$$

Where: S is the sliding surface or error (S = X^*− X), with:

$$S_\Omega = \xi = \Omega_{ref} - \Omega \quad (14)$$

β_1, β_2, and β_3 are the positive gains.

This approach, which we will call the FTOSMC command for convenience, will be applied to the DSIM engine in order to control its instability. Figure 1 illustrates the proposed third-order sliding mode control (TOSMC) strategy. The command input of the designed FTOSMC controller comprises three inputs given by (15)-(18).

$$U(t) = U_1(t) + U_2(t) + U_3(t) \quad (15)$$

$$U_1(t) = \beta_1 . \sqrt{|S_\Omega|} . U_f(S_\Omega) \quad (16)$$

$$U_2(t) = \beta_2 . \int U_f(S_\Omega) dt \quad (17)$$

$$U_3(t) = \beta_3 . U_f(S_\Omega) \quad (18)$$

The (19) shows the output of the proposed FTOSM method:

$$U(t) = \beta_1 . \sqrt{|S_\Omega|} . U_f(S_\Omega) + \beta_2 . \int U_f(S_\Omega) dt + \beta_3 . U_f(S_\Omega) \quad (19)$$

Figure 2 shows a block diagram of the fuzzy third-order sliding mode control (FTOSMC) strategy.

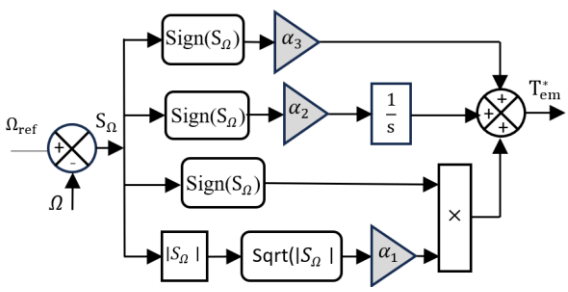

Figure 1. The TOSMC strategy

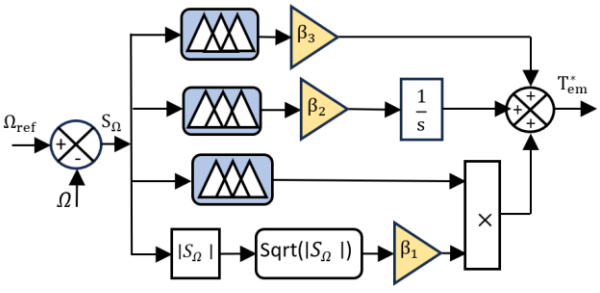

Figure 2. The FTOSMC strategy

To generate the fuzzy system, we defined seven fuzzy sets, which are represented by the triangular membership functions shown in Figures 3 and 4, respectively. These sets are (NB, NM, NS, ZE, PS, PM, PB). The choice of the triangular shape of the fuzzy membership functions used is justified by the ease of their design and allows for better adjustment of their geometric parameters, which offers a better adaptation of this sliding fuzzy controller to the operating conditions of the machine. It is also crucial to emphasize that

the transition of the different fuzzy inference rules is executed more judiciously, thanks to the smooth shape of these membership functions. The fuzzy inference table adopted uses the Mamdani model, which is defined by the minimum, which is symbolized by "min" to calculate the degree μ(ΔS) with respect to each rule, for example, [μ(ΔS) = min μ(s), μ(ṡ)]. The normalized output function is represented by the following relation:

$$U_f(S_\Omega) = \frac{\sum_{i=1}^{n} \mu(\Delta s)\Delta s}{\sum_{i=1}^{n}(\Delta s)} \quad (20)$$

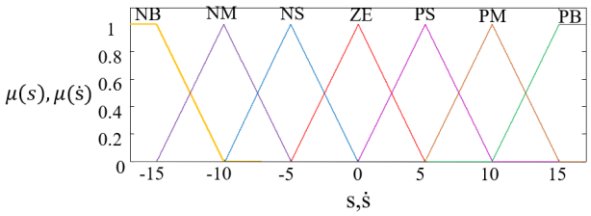

Figure 3. Membership functions for input values s,$\dot{s}$

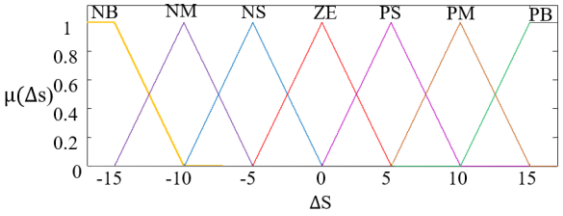

Figure 4. Membership functions for output value $\Delta(s)$

6. IMPLEMENTATION OF MOA-FTOSMC TECHNIQUE

The different stages of the MOA are represented by the flowchart in Figure 5, where g-best is the global optimal solution and p-best is the optimal location [26]. Table 1 presents the performance comparison of control strategies during speed reversal. The input and output parameters with their corresponding values of the MOA are illustrated in Table 2.

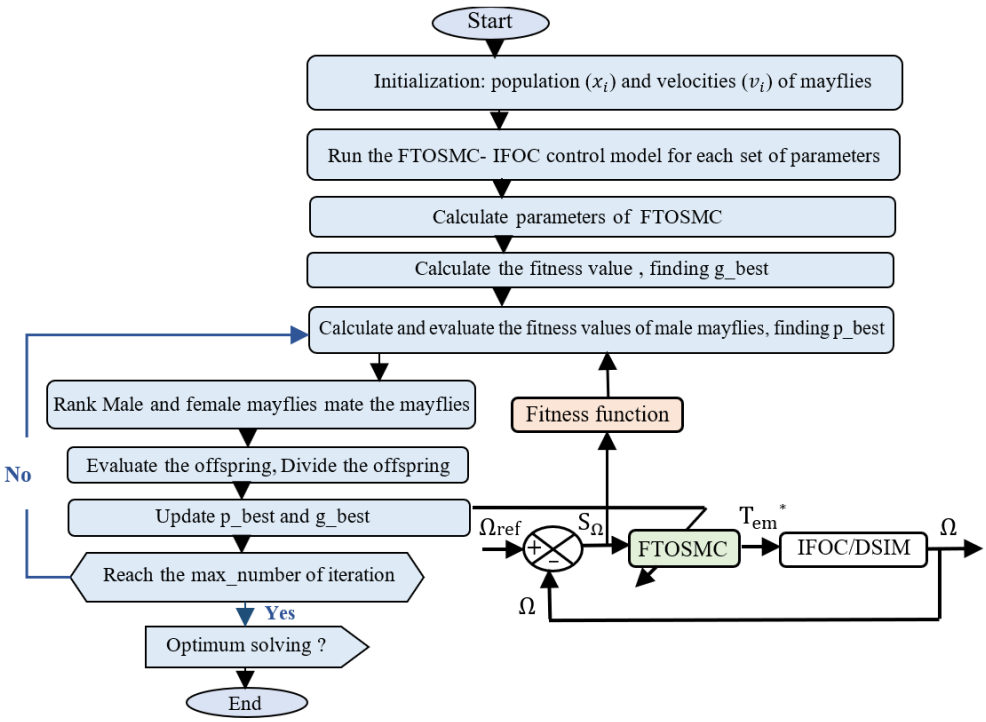

Figure 5. Flowchart illustrating the implementation of the MOA

Table 2. MOA parameter setting

Parameter	Meaning	Value	Parameter	Meaning	Value
MaxIter	Random flight coefficient	20	a1/a2/a3	Max number of iterations	1/1.5/1.5
NPop	Number of males	10	Beta	Learning coefficient	2
NPopf	Number of females	10	D	Distance sight coefficient	5
g	Gravitational coefficient	0.98	fl	Coefficient of nuptial dance	1
gdamp	Inertia damping ratio	1	Dance damp/fl damp	The damping ratio	0.8/ 0.99

7. RESULTS ANALYSIS AND DISCUSSION

To illustrate the contribution made to the performance of the IFOC control on DSIM, the MOA is used to adjust the best proportional and integral gains of the speed regulator. These gains are reinforced by robust techniques that allow the system to judiciously follow its reference speed. The techniques considered in this case are, respectively, SOSMC, TOSMC, and finally FTOSMC. It is crucial to perform a simulation of the system using Simulink under the MATLAB environment to compare the three strategies and validate the performance and robustness of each regulator under different load and disturbance conditions. This comparison helps determine the most appropriate technique for optimal system operation. The block diagram of this simulation is presented in Figure 6.

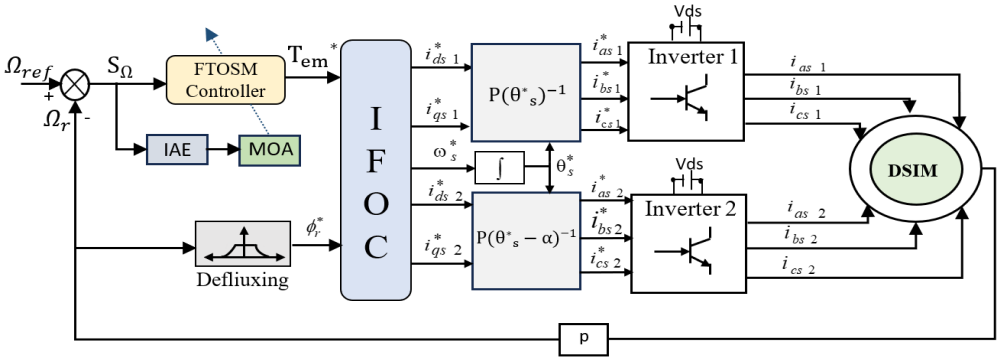

Figure 6. Block diagram of the (IFOC) combined with MOA-FTOSMC for the (DSIM)

Figure 7 illustrates the system's response to two key events: a reference speed change from 300 rad/s to 40 rad/s at t = 2.5 s, and the application of a +20 N.m load torque disturbance at t = 2 s. From the zoomed-in view of the three response curves, the reference speed tracking performance of each controller can be effectively evaluated. The MOA-SOSMC controller exhibits a significant deviation at the moment of disturbance and a noticeable delay in reaching the new reference speed, indicating weaker disturbance rejection and slower dynamic response. The MOA-TOSMC controller performs better, with improved disturbance handling and faster convergence to the new speed, though some delay is still evident. In contrast, the MOA-FTOSMC controller demonstrates clearly superior performance, exhibiting robust disturbance rejection at t = 2 s and rapid, accurate tracking of the reference speed at t = 2.5 s. These results confirm the MOA-FTOSMC's effectiveness in achieving both high-speed response and strong robustness against external disturbances.

The tests conducted under speed and load variations confirm that this innovative hybrid approach combines (MOA-FTOSMC), (MOA-TOSMC), and (MOA-SOSMC). MOA-FTOSMC is both promising and highly effective. It consistently delivers improved and reliable performance in terms of response time, rise time, settling time, overshoot, disturbance rejection, and steady-state error reduction.

Figure 8 clearly shows that the stator current of the MOA-FTOSMC technique exhibits less chattering and ripple, while maintaining its sinusoidal shape more effectively. Similarly, Figure 9 illustrates the electromagnetic torque profile under a speed variation at t = 2.5 s and the application of a 20 Nm load torque at t = 2 s. In this scenario, the MOA-FTOSMC strategy (depicted in blue) effectively tracks the load command, exhibiting only minor overshoots and a significant reduction in chattering compared to the other two methods: MOA-SOSMC and MOA-TOSMC. It is also noteworthy that the MOA-TOSMC strategy (shown in green) outperforms the MOA-SOSMC approach (in red), delivering more stable and satisfactory torque behavior.

Figure 10 depicts the variations of the rotor flux components in the q- and d-axis reference frames. As expected, the q-axis component remains at zero, while the d-axis component closely tracks its reference value of 1 Wb. For the MOA-FTOSMC controller, slight ripples appear during speed changes, but overall performance is superior to the other two techniques, which show more significant deviations.

Total harmonic distortion (THD) quantifies the distortion of electrical signal waveforms relative to their fundamental frequency components. A lower THD value reflects higher efficiency and improved system performance. This is clearly demonstrated by the MOA-FTOSMC approach, as illustrated in Figure 11, which shows the THD of the stator current. The MOA-FTOSMC achieves a THD of approximately 15.26%, significantly lower than those of the other two strategies: MOA-TOSMC at 18.84% and MOA-SOSMC at 20.42%. Elevated THD values result in distorted current and voltage waveforms, causing torque and power irregularities that can ultimately compromise system reliability. Table 3 presents the performance of the MOA-FTOSMC controller.

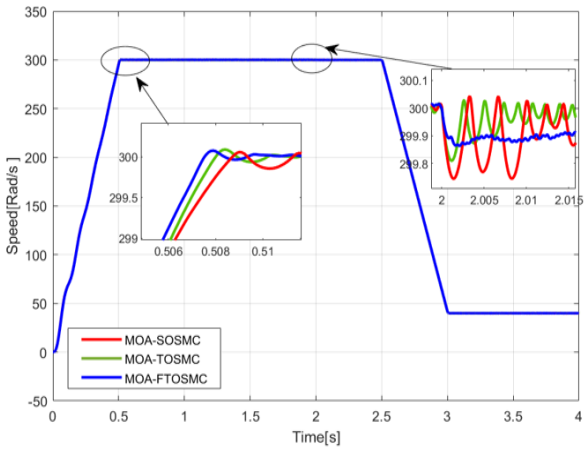

Figure 7. Speed variation from 300 rad/s to 40 rad/s

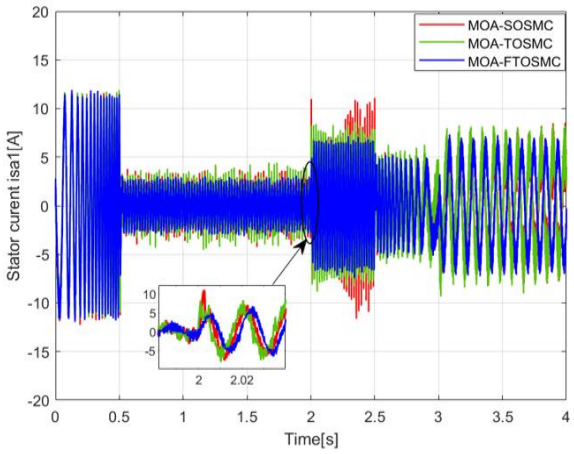

Figure 8. Torque with speed variation from 300 rad/s to 40 rad/s

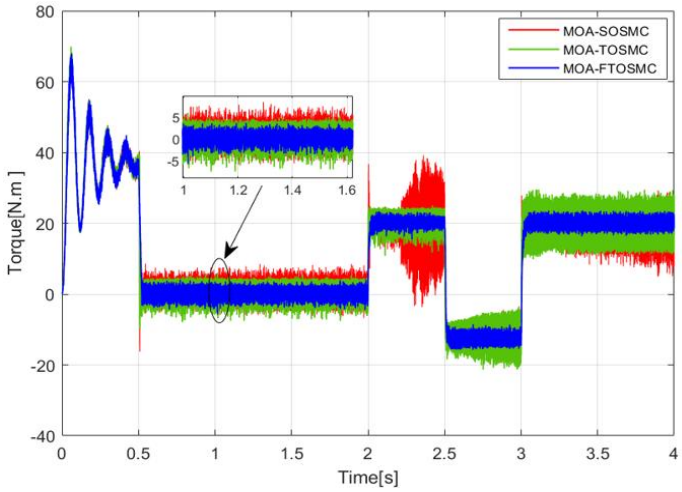

Figure 9. Electromagnetic torque response during speed variation from 300 rad/s to 40 rad/s

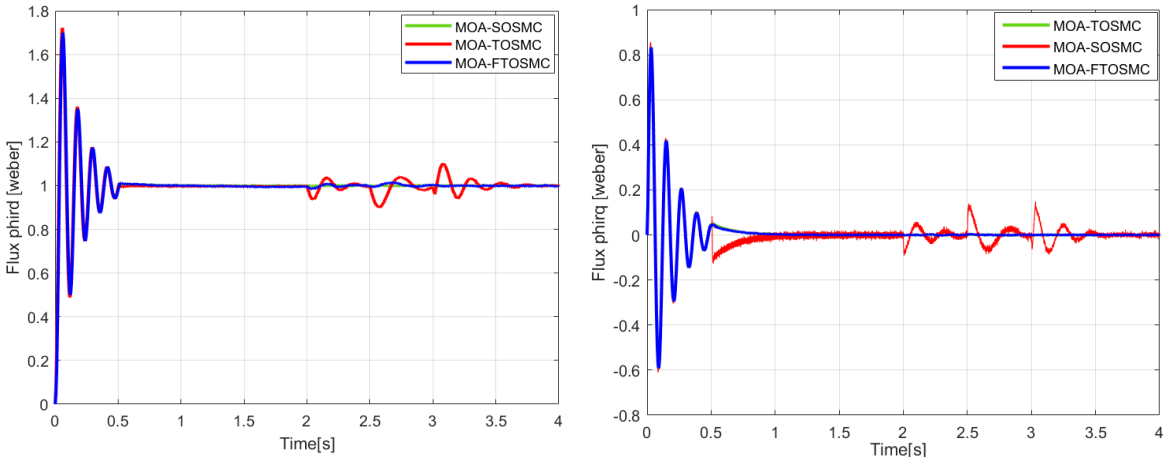

Figure 10. Rotor flux components: d-axis flux and q-axis flux

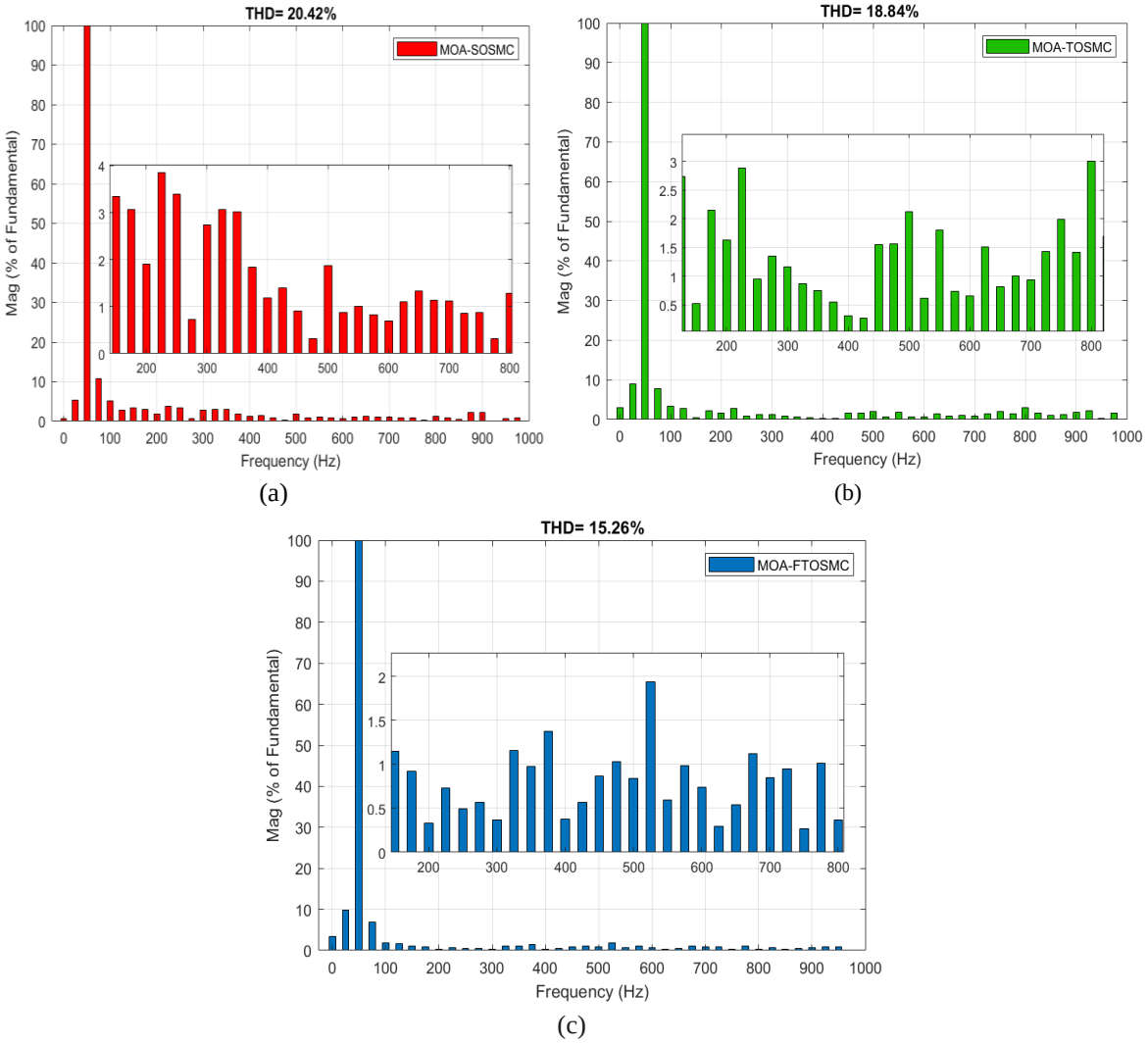

Figure 11. FFT analysis of the stator current for (a) MOA-SOSMC, (b) MOA-TOSMC, and (c) MOA-FTOSMC

Figure 12 provides a detailed analysis of the fitness function evolution, showcasing the effectiveness of the MOA when combined with the three studied approaches. The visualization highlights significant differences in performance:

a) The curve represented by the black dotted line corresponds to the MOA-FTOSMC technique, identified by the coordinates (x = 14.03, y = 0.00141). This approach achieves near-zero values on the x-axis and converges toward an optimal solution, stabilizing by the fourth iteration. This behavior signifies the remarkable and satisfactory performance of the training system, outperforming the other strategies.

b) In contrast, the other two approaches exhibit slower convergence and less effective optimization:
   - MOA-SOSMC: Represented by the red curve, with coordinates (x = 19.11, y = 0.003667), it demonstrates prolonged exploration of the search space without achieving desired convergence.
   - MOA-TOSMC: Depicted by the blue curve, with coordinates (x = 16.24, y = 0.002747), it also struggles to optimize efficiently, resulting in suboptimal parameter selection.

These observations underscore the superiority of the MOA-FTOSMC technique, which rapidly and efficiently converges to the optimal solution, thereby ensuring significantly enhanced system performance compared to the other two strategies. According to the data in Table 4.

Table 3. Performance of the MOA-FTOSMC controller

Input scaling Factor optimized ke	Input scaling Factor optimized kd	Output scaling Factor optimized β_1	Output scaling Factor optimized β_2	Output scaling Factor optimized β_3
10.220	4.376	8.4303	6.8464	6.7788

Table 4. Performance comparison of the three control approaches

Approach	MOA-SOSMC	MOA-TOSMC	MOA-FTOSMC
Robustness	Average	Satisfactory	High
Chattering	Less reduced	Reduced	very reduced
Dynamic Responses	Unsatisfactory	Satisfactory	high
Rising time of the speed (s)	0.5062	0.5061	0.5057
Harmonic of stator current (%)	20.42%	18.84%	15.26%
Transient performance of the speed	unsatisfactory	good	high

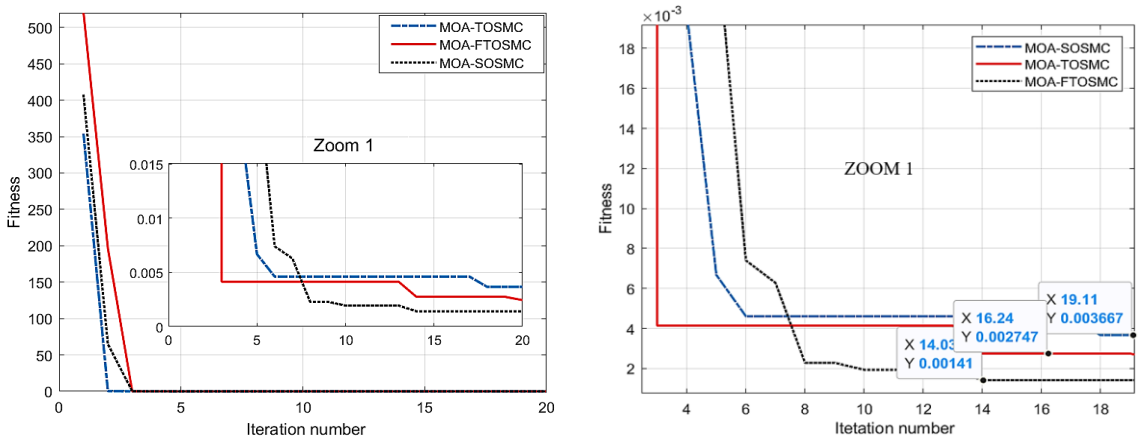

Figure 12. Evolution of the fitness function for the (MOA) combined with the three control approaches

8. CONCLUSION

Due to the inherent complexity and nonlinearity of electric drive systems, modeling and simulation are essential for effective fault detection across various operating conditions, including speed variations, reversals, and changing loads. In this study, we integrate advanced control strategies, fuzzy logic, sliding mode control, and (MOA) to tackle these challenges. The fuzzy sliding mode controller enhances performance by refining control actions based on both the error and its derivative, while the MOA efficiently selects speed regulator gains through adaptive exploration of the search space, achieving rapid convergence to optimal solutions with fewer iterations. Simulation results demonstrate improved system stability, enhanced disturbance rejection, and reduced overshoot attributed to fuzzy logic. Moreover, the third-order sliding mode control significantly diminishes the chattering effect while boosting overall robustness. This hybrid approach presents a promising advancement for the automotive industry, contributing to greater energy efficiency and smoother speed regulation.

FUNDING INFORMATION

This work was funded by the Electrical Traction Systems Laboratory Batna (LSTEB), University of Batna 2 (Mostefa Benboulaid), Algeria.

AUTHOR CONTRIBUTIONS STATEMENT

This journal uses the Contributor Roles Taxonomy (CRediT) to recognize individual author contributions, reduce authorship disputes, and facilitate collaboration.

Name of Author	C	M	So	Va	Fo	I	R	D	O	E	Vi	Su	P	Fu
Rahma Belkaid	✓	✓	✓	✓	✓	✓		✓	✓	✓			✓	
Lamia Youb		✓		✓	✓	✓		✓	✓	✓	✓	✓	✓	
Farid Naceri		✓	✓	✓						✓		✓		
Ghoulem Allah Boukhalfa	✓	✓	✓	✓				✓		✓	✓			

C : **C**onceptualization
M : **M**ethodology
So : **So**ftware
Va : **Va**lidation
Fo : **Fo**rmal analysis
I : **I**nvestigation
R : **R**esources
D : **D**ata Curation
O : Writing - **O**riginal Draft
E : Writing - Review & **E**diting
Vi : **Vi**sualization
Su : **Su**pervision
P : **P**roject administration
Fu : **Fu**nding acquisition

CONFLICT OF INTEREST STATEMENT

Authors state no conflict of interest.

DATA AVAILABILITY

We confirm that the data supporting the findings of this study are available within the article and its supplementary materials.

REFERENCES

[1] K. Hamitouche, S. Chekkal, H. Amimeur, and D. Aouzellag, "A new control strategy of dual stator induction generator with power regulation," *Journal Européen des Systèmes Automatisés*, vol. 53, no. 4, pp. 469–478, Sep. 2020, doi: 10.18280/jesa.530404.

[2] W. Ma, L. Xi, Y. Zhang, Z. He, X. Zhang, and Z. Cai, "Design and comparison of linear induction motor and superconducting linear synchronous motor for electromagnetic launch," in *2021 13th International Symposium on Linear Drives for Industry Applications (LDIA)*, IEEE, Jul. 2021, pp. 1–5. doi: 10.1109/LDIA49489.2021.9505785.

[3] E. Benyoussef and S. Barkat, "Five-level direct torque control with balancing strategy of double star induction machine," *International Journal of Systems Applications, Engineering & Development*, vol. 14, pp. 116–123, Dec. 2020, doi: 10.46300/91015.2020.14.16.

[4] H. Rahali, S. Zeghlache, and L. Benalia, "Adaptive field-oriented control using supervisory type-2 fuzzy control for dual star induction machine," *International Journal of Intelligent Engineering and Systems*, vol. 10, no. 4, pp. 28–40, Aug. 2017, doi: 10.22266/ijies2017.0831.04.

[5] R. Belal, M. Flitti, And M. L. Zegai, "Tuning of PI speed controller in direct torque control ofdual star induction motor based on genetic algorithms and neuro-fuzzy schemes," *Revue Roumaine des Sciences Techniques — Série Électrotechnique Et Énergétique*, vol. 69, no. 1, pp. 9–14, Apr. 2024, doi: 10.59277/RRST-EE.2024.1.2.

[6] E. Terfia, S. E. Rezgui, S. Mendaci, H. Gasmi, and H. Benalla, "Optimal fractional order proportional integral controller for dual star induction motor based on particle swarm optimization algorithm," *Journal Européen des Systèmes Automatisés*, vol. 56, no. 2, pp. 345–353, Apr. 2023, doi: 10.18280/jesa.560220.

[7] X. Fan, W. Sayers, S. Zhang, Z. Han, L. Ren, and H. Chizari, "Review and classification of bio-inspired algorithms and their applications," *Journal of Bionic Engineering*, vol. 17, no. 3, pp. 611–631, May 2020, doi: 10.1007/s42235-020-0049-9.

[8] G. Boukhalfa, S. Belkacem, A. Chikhi, and S. Benaggoune, "Genetic algorithm and particle swarm optimization tuned fuzzy PID controller on direct torque control of dual star induction motor," *Journal of Central South University*, vol. 26, no. 7, pp. 1886–1896, Jul. 2019, doi: 10.1007/s11771-019-4142-3.

[9] Q. Du and H. Zhu, "Dynamic elite strategy mayfly algorithm," *PLOS ONE*, vol. 17, no. 8, p. e0273155, Aug. 2022, doi: 10.1371/journal.pone.0273155.

[10] K. Zervoudakis and S. Tsafarakis, "A mayfly optimization algorithm," *Computers & Industrial Engineering*, vol. 145, p. 106559, Jul. 2020, doi: 10.1016/j.cie.2020.106559.

[11] L. Youb, S. Belkacem, F. Naceri, M. Cernat, And L. G. Pesquer, "Design of an adaptive fuzzy control system for dual star induction motor drives," *Advances in Electrical and Computer Engineering*, vol. 18, no. 3, pp. 37–44, 2018, doi: 10.4316/AECE.2018.03006.

[12] J. D. Allan and A. S. Flecker, "The mating biology of a mass-swarming mayfly," *Animal Behaviour*, vol. 37, pp. 361–371, Mar. 1989, doi: 10.1016/0003-3472(89)90084-5.

[13] T. Tudorache, I. D. Ilina, and L. Melcescu, "Parameters estimation of an induction motor using optimization algorithms," *Revue Roumaine des Sciences Techniques Serie Electrotechnique et Energetique*, vol. 61, no. 2, pp. 121–125, 2016.

[14] F. Z. Tria, K. Srairi, M. T. Benchouia, B. Mahdad, and M. E. H. Benbouzid, "An hybrid control based on fuzzy logic and a second order sliding mode for mppt in wind energy conversion systems," *International Journal on Electrical Engineering and Informatics*, vol. 8, no. 4, pp. 711–726, Dec. 2016, doi: 10.15676/ijeei.2016.8.4.1.

[15] E. Zakeri, S. A. Moezi, and M. Eghtesad, "Optimal interval type-2 fuzzy fractional order super twisting algorithm: A second order sliding mode controller for fully-actuated and under-actuated nonlinear systems," *ISA Transactions*, vol. 85, pp. 13–32, Feb. 2019, doi: 10.1016/j.isatra.2018.10.013.

[16] N. Layadi *et al.*, "Fault-tolerant control based on sliding mode controller for double-star induction machine," *Arabian Journal for Science and Engineering*, vol. 45, no. 3, pp. 1615–1627, Mar. 2020, doi: 10.1007/s13369-019-04120-1.

[17] H. Benbouhenni, "Amelioration effectiveness of torque and rotor flux control applied to the asynchronous generator for dual-rotor wind turbine using neural third-order sliding mode approaches," *International Journal of Engineering*, vol. 35, no. 3, pp. 517–530, 2022, doi: 10.5829/IJE.2022.35.03C.04.

[18] S. Mahfoudhi, M. Khodja, and F. Mahroogi, "A second-order sliding mode controller tuning employing particle swarm optimization," *International Journal of Intelligent Engineering and Systems*, vol. 13, no. 3, pp. 212–221, Jun. 2020, doi: 10.22266/ijies2020.0630.20.

[19] M. Morawiec, P. Strankowski, A. Lewicki, J. Guzinski, and F. Wilczynski, "Feedback control of multiphase induction machines with backstepping technique," *IEEE Transactions on Industrial Electronics*, vol. 67, no. 6, pp. 4305–4314, Jun. 2020, doi: 10.1109/TIE.2019.2931236.

[20] I. Yaichi, A. Semmah, P. Wira, and Y. Djeriri, "Super-twisting sliding mode control of a doubly-fed induction generator based on the SVM strategy," *Periodica Polytechnica Electrical Engineering and Computer Science*, vol. 63, no. 3, pp. 178–190, Jun. 2019, doi: 10.3311/PPee.13726.

[21] E. Terfia, S. Mendaci, S. E. Rezgui, H. Gasmi, and W. Kantas, "Optimal third-order sliding mode controller for dual star induction motor based on grey wolf optimization algorithm," *Heliyon*, vol. 10, no. 12, p. e32669, Jun. 2024, doi: 10.1016/j.heliyon.2024.e32669.

[22] F. Mazouz, S. Belkacem, and G. Boukhalfa, "Second order sliding mode control based DPC of DFIG Using SVM," in *Artificial Intelligence and Heuristics for Smart Energy Efficiency in Smart Cities*, 2022, pp. 743–750. doi: 10.1007/978-3-030-92038-8_75.

[23] F. Berrezzek and A. Benheniche, "Backstepping based nonlinear sensorless control of induction motor system," *Journal Européen des Systèmes Automatisés*, vol. 54, no. 3, pp. 495–502, Jun. 2021, doi: 10.18280/jesa.540313.

[24] D. Zellouma, H. Benbouhenni, and Y. Bekakra, "Backstepping control based on a third-order sliding mode controller to regulate the torque and flux of asynchronous motor drive," *Periodica Polytechnica Electrical Engineering and Computer Science*, vol. 67, no. 1, pp. 10–20, Jan. 2023, doi: 10.3311/PPee.20333.

[25] H. Benbouhenni and N. Bizon, "Third-order sliding mode applied to the direct field-oriented control of the asynchronous generator for variable-speed contra-rotating wind turbine generation systems," *Energies*, vol. 14, no. 18, p. 5877, Sep. 2021, doi: 10.3390/en14185877.
[26] G. Lei, X. Chang, Y. Tianhang, and W. Tuerxun, "An improved mayfly optimization algorithm based on median position and its application in the optimization of pid parameters of hydro-turbine Governor," *IEEE Access*, vol. 10, pp. 36335–36349, 2022, doi: 10.1109/ACCESS.2022.3160714.

BIOGRAPHIES OF AUTHORS

Rahma Belkaid was born in Batna, Algeria. She obtained a master's degree from the University of Mustafa Ben Boulaaid Batna 2, Algeria, specializing in electrical systems control. She is currently enrolled in her third year of an LMD doctoral program at the University of Batna 2. She is a member of the Electrical Traction Systems Laboratory Batna (LSTEB). She can be contacted at email: rahma.belkaid@univ-batna2.dz.

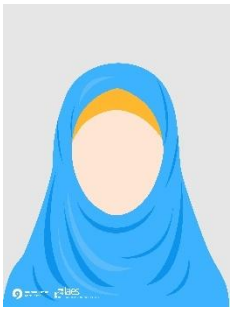

Lamia Youb was born in Batna, Algeria. She received the B.Sc. Degree in electrical engineering from the University of Batna, Algeria in 2002, and she got her Ph.D. degree in electrical engineering from Politehnica University of Bucharest, Romania, 2007. After graduation, she joined the University of Batna 2, Algeria, where she is a professor at the science and engineering faculty. Her current research area includes advanced control techniques, the application of fuzzy logic, renewable energy, and digital signal processing. She can be contacted at email: l.youb@univ-batna2.dz.

Farid Naceri was born in Algeria. He received his B.S. and M.S. degrees in electrical engineering from the University of Batna, and his Ph.D. degree in Automatic Control. He is a professor at the Department of Electrical Engineering, University of Batna 2. He is a member of the Electrical System Traction Laboratory (LSTE). His current research interests are control of AC machines, adaptive and optimal control, power electronics, and identification. He can be contacted at email: f.naceri@univ-batna2.dz.

Ghoulem Allah Boukhalfa was born in Ain Touta – Batna-, Algeria. He obtained his Ph.D. degree in electromechanics in 2020. Currently, he is a teacher of electrical engineering and a member of the LAB Laboratory, Electromechanical Department, University of Mustafa Ben Boulaaid, Batna 2, Algeria. His research interests include the application of robust control for optimizing generation systems and wind turbine systems' intelligent control. He can be contacted at email: ghoulem1987@gmail.com.